General Disclaimer

One or more of the Following Statements may affect this Document

- This document has been reproduced from the best copy furnished by the organizational source. It is being released in the interest of making available as much information as possible.

- This document may contain data, which exceeds the sheet parameters. It was furnished in this condition by the organizational source and is the best copy available.

- This document may contain tone-on-tone or color graphs, charts and/or pictures, which have been reproduced in black and white.

- This document is paginated as submitted by the original source.

- Portions of this document are not fully legible due to the historical nature of some of the material. However, it is the best reproduction available from the original submission.

NASA Technical Memorandum 79040

HIGH VELOCITY BURNER RIG OXIDATION AND THERMAL FATIGUE BEHAVIOR OF Si_3N_4- AND SiC-BASE CERAMICS TO 1370° C

William A. Sanders and James R. Johnston
Lewis Research Center
Cleveland, Ohio

November 1978

SUMMARY

Hot pressed Si_3N_4, reaction sintered Si_3N_4 of two types and siliconized SiC were exposed in a Mach 1 gas velocity burner simulating a turbine engine environment. Test materials were selected on the basis of potential for gas turbine usage, near-net-shape fabricability and commercial/domestic availability. Cyclic tests were conducted on simulated vane shape specimens for up to 250 cycles (50 hr at temperatures of 1205°, 1260°, 1315°, and 1370° C. Each cycle consisted of a 12 minute heating period and a 3 minute still air cooling period. Vane specimens were evaluated and compared periodically on the basis of weight change, surface change, fluorescent penetrant inspection, and thermal fatigue behavior.

All six hot pressed Si_3N_4 vanes, which represented two batches of material, survived 250 cycle exposures at 1260°, 1315°, and 1370° C without cracking and with only slight weight losses.

One reaction sintered Si_3N_4 material was clearly superior to the other reaction sintered Si_3N_4 material in regards to thermal fatigue resistance and oxidation weight gain. Out of nine vanes of one reaction sintered Si_3N_4 material tested, seven vanes survived 250 cycle exposure versus one vane survivor (out of nine) for the other reaction sintered Si_3N_4. The differences in behavior of these two materials were related to vane specimen machined surface condition, high variability in density and open porosity within vanes and batch to batch, high open porosity, and pore size.

The behavior of the siliconized SiC material was found to correlate with the amount of free silicon present in the vane specimens. All three vane specimens of the material batch with the lowest amount of free silicon survived 250 cycle exposures at 1205°, 1260°, and 1315° C. Only one of the remaining six vanes survived 250 cycles. Thermal fatigue failures and oxidation weight gain correlated with the degree of exudation of molten silicon-base eutectic.

E-9842

INTRODUCTION

This work was performed in cooperation with the Air Force Materials Laboratory (AFML) in support of an AFML contract with Illinois Institute of Technology Research Institute (IITRI) (ref. 1). The results of the Lewis Research Center burner rig work reported here on the oxidation and thermal fatigue behavior of four Si_3N_4- and SiC-base ceramic materials will supplement extensive mechanical and physical property determinations by IITRI, and determinations of phase composition, microstructure, and chemical analysis by AFML on the four ceramic materials. The AFML contract calls for a thorough property characterization of four Si_3N_4- and SiC-base ceramic materials to provide data for turbine engine designers. This data package will fill a requirement for an independent evaluation and in depth comparison of materials where the experimental testing is accomplished using the same techniques and test parameters. Three batches of each material were to be evaluated in order to determine batch-to-batch variation and reproducibility. The materials were selected on the basis of AFML-judged potential, near-net-shape fabricability and commercial/domestic availability.

In addition to past efforts at the Lewis Research Center (refs. 2 and 3), other organizations have also screened ceramic materials and have gone on to rig testing Si_3N_4- and SiC-base material parts for specific turbine engine applications. The most notable of these ceramic testing activities have been carried out by Ford Motor Company (refs 4 and 5) for a small vehicular gas turbine and by Westinghouse Research and Development Center for a large stationary gas turbine for electric power generation (ref. 6). Both of these activities have been funded by the Advanced Research Projects Agency in an iterative design and materials development program initiated July 1971. Hot pressed Si_3N_4, reaction sintered Si_3N_4 and SiC containing free silicon have been found to be the ceramics of widest applicability for high temperature structural applications.

In the past Lewis work we have used a Mach 1 burner to screen a variety of ceramic materials in simple rod geometry (ref. 2), and to evaluate Si_3N_4- and SiC-base materials in a simulated vane shape geom-

etry (ref. 3). The vane shape incorporates a simulated airfoil leading edge allowing the material to experience severe thermal stresses. The four Si_3N_4- and SiC-base ceramic materials selected by AFML were tested in the vane shape.

The burner used for the evaluation of the materials was operated at a hot gas velocity of Mach 1 with Jet A a kerosene-type fuel. Vanes were tested individually by cyclic exposure to the burner rig Mach 1 hot gas stream. Vane leading edge test temperatures of 1205°, 1260°, 1315°, and 1370° C were employed. Maximum target exposure established by AFML for any vane in this investigation was 250 twelve-minute cycles (approximately 50 hr at test temperature). Materials and material batches were compared as to weight change, surface change, thermal fatigue behavior, and by fluorescent penetrant inspection where practical.

MATERIALS

Table I lists the four ceramic materials evaluated along with the number of batches and total number of vanes involved. The three materials with the NC designation were procured from Norton Company, Worcester, Massachusetts. The KBI designation refers to Kawecki-Berylco Industries who is the United States licensee for Advanced Materials Engineering of Great Britain. The KBI reaction sintered Si_3N_4 evaluated in this program was manufactured in Great Britain. KBI is now manufacturing reaction sintered Si_3N_4 in the United States.

NC-132 Hot Pressed Si_3N_4

Although not of near-net-shape fabricability, two batches of NC-132 hot pressed Si_3N_4 were included in the program because considerable data has been generated on this material and it is widely considered a standard or baseline for comparisons. This fully dense material is produced from fine Si_3N_4 powder which is milled with a small amount of MgO additive which acts as a densification aid during the hot pressing consolidation. Test vanes were prepared by Norton Company by diamond grinding of blanks which were diamond cut from hot pressed billets.

NC-350 Reaction Sintered Si_3N_4

For this program, 75 to 81 percent dense NC-350 reaction sintered Si_3N_4 vanes were diamond machined by Norton Company from three batches of RS Si_3N_4 plates approximately 1/2 cm in thickness. These plates were produced by cold pressing high purity silicon powder and then nitriding the cold pressed bodies to form Si_3N_4. Although not taken advantage of here, this material offers the near-net-shape forming of parts which would then require minimal diamond machining.

KBI Reaction Sintered Si_3N_4

Test vanes of this material 74 to 84 percent dense were made by the supplier by a fabrication route taking some advantage of the capability for near-net-shape forming of parts. Test vane shapes were first cut from three batches of blocks of cold pressed silicon powder. These shapes were then nitrided to form Si_3N_4, and the shapes were finished by diamond machining only as required to meet required dimensions.

NC-435 Siliconized SiC

This material also has near-net-shape fabricability and does not require hot pressing for consolidation. Slip cast blanks of fine SiC powder were prefired and densified by infiltration with silicon. About 20 percent silicon by volume is present. Test vanes were diamond ground by Norton Company, and had densities in the range 97 to 99 percent of the theoretical density for a SiC + 20 percent Si body. Open porosity was negligible.

Spectrographic analyses and X-ray diffraction analyses of the four materials were performed by AFML (ref. 7) and are presented in tables II and III, respectively. For chemical analysis, at least two representative samples from each material batch were analyzed and an average value is given in table II. Also given is an average value for the total numbers of batches as well as the major impurities listed in descending concentration. The NC-132 hot pressed Si_3N_4 has the

highest impurity level due to the presence of approximately 2 percent tungsten and 0.4 magnesium. The tungsten contamination is likely the result of milling Si_3N_4 powder with tungsten carbide media. The oxygen level for NC-132 is also much higher than for the reaction sintered materials. Of the two reaction sintered Si_3N_4 materials, the Norton NC-350 material is somewhat purer than the Kawecki-Berylco material, with the NC-435 reaction sintered SiC purity falling in between. Iron and aluminum are major impurities in all cases. The phases present in all batches of the four materials are presented in table III. Of chief note is the difference in the relative amounts of alpha and beta Si_3N_4 for the two reaction sintered Si_3N_4 materials.

SPECIMENS AND APPARATUS

Vane Specimens

The vane specimen geometry and dimensions are shown in figure 1. One long edge (hereafter referred to as the leading edge) of the vane tapers as shown in figure 1 to a radius of approximately 0.08 cm. In test, the Mach 1 hot gas stream impinges directly on this leading edge. The tapered leading edge constrained by the more massive (and slower in thermal response) body of the vane leads to thermal stresses during thermal cycling. Due to thickness limitations in the production of NC-350 reaction sintered Si_3N_4, the vanes of this material were only 0.42 cm thick instead of the standard 0.64 cm thickness. For this reason, the thermal stresses generated during the heating and cooling cycles were probably somewhat lower for the NC-350 material.

For the porous reaction sintered Si_3N_4 vanes the percent theoretical density and the percent open porosity based on IITRI measurements (ref. 8) are given in table IV. Also given in this table are alpha -Si_3N_4 to beta -Si_3N_4 ratios determined by X-ray diffraction analysis performed at Lewis. The variations in density and porosity both within batch and from batch to batch are somewhat less for the NC-350 material than for the KBI material. The alpha/beta weight ratios show considerable batch to batch variation for both materials.

As previously stated the NC-132 and NC-435 materials were essentially 100 percent dense.

Vane surface appearance. - Low power (×30) binocular inspection of the NC-132 vanes showed them to be of the best overall surface condition of the four vane test materials. The NC-435 vanes displayed some permanent surface staining but vane surfaces were generally in good condition. The NC-350 vane surfaces were less uniform than the surfaces of NC-132 or NC-435 when batch-to-batch comparisons were made. Although within batches the NC-350 vanes were of uniform gray coloration, there were color differences in the shades of gray between batches as illustrated in figure 2. The Batch 2 vanes were a lighter gray than the Batch 3 vanes. The Batch 1 NC-350 vanes not shown were very similar in appearance to the Batch 3 vanes. The striated appearance of vanes 1 and 3 of NC-350 Batch 2 are believed due to some machining anomaly. At ×30 magnification the texture of the dark and light bands appeared the same. The other side of the striated vanes was a uniform shade of gray the same as vane 2 of Batch 2. The KBI vanes of reaction sintered Si_3N_4 also displayed considerable batch-to-batch color variation, and also within-batch and within-vane color variations as shown in figure 3. For Batch 1, the major surfaces, and particularly the leading edges and the flats opposite the leading edges, were considerably darker than the corresponding surfaces of Batch 3 which were light gray. The KBI Batch 2 vanes not shown were slightly darker than the Batch 3 vanes. Several of the KBI vanes had deep grinding marks and areas of high porosity. These features likely follow from the way in which the KBI vanes were made. The vane shapes were cut from a block of cold pressed silicon powder, and after nitriding were finished by diamond grinding only as necessary to meet required dimensions. Thus, some vane surfaces were in the less perfect as-nitrided condition as opposed to the much smoother surface resulting from diamond grinding.

For both reaction sintered Si_3N_4 materials it was noted that the darkest batch of vanes had the highest densities and the lowest open porosities.

Burner rig. - A schematic of the Mach 1 burner rig is shown in figure 4. The apparatus was operated with Jet A fuel at a jet gas velo-

city of Mach 1 at the gas temperature and specimen temperature ranges included in figure 4. Ceramic vanes were tested singly with the leading edges facing the 2-inch diameter burner nozzle as shown. A section of ceramic-coated metal pipe positioned behind the test vane acted as a radiator to augment the heat input to the vane. The test vane holder was a new two-piece design which included springs for clamping and a platinum compliant layer. The platinum compliant layer consisted of two pieces of 0.25 mm platinum sheet which fitted around the retained length of the test vane. Compressive loads applied through a spring mechanism held the vane effectively, and, chipping due to loosening in the holder, which was a problem in a previous program (ref. 3), was eliminated.

PROCEDURE

Temperature

For temperature calibration, a chromel-alumel thermocouple with a 3 mm diameter, roughly spherical, hot junction took the place of a ceramic test vane in the burner rig. The thermocouple hot junction was fixed into a position coincident with the intersection of the horizontal burner nozzle center line and a vertical line defining the position of a test vane leading edge. The burner was then operated at Mach 1 under conditions which heated the heavy thermocouple bead to equilibrium temperatures of 1205°, 1260°, 1315°, and 1370° C as measured by the thermocouple E.M.F. generated. For each thermocouple temperature, a corresponding optical measurement was made by sighting on the glowing thermocouple bead with a disappearing filament optical pyrometer. With this calibration, the optical pyrometer was then routinely used to establish the required ceramic vane specimen leading edge temperature. Emittance corrections were not necessary since the emittances of oxidized chromel-alumel and oxidized Si_3N_4 and SiC are very similar. Test temperatures were judged to be maintained within $\pm 10^{\circ}$ C.

A radiation pyrometer focused on the test specimen automatically controlled the specimen temperature.

Exposure cycle. - A test cycle was 15 minutes in length, consisting of a 12 minute heating period and a 3-minute still air cooling period. The exposure goal for each test vane was 250 cycles. To begin heating or cooling, the test vane was rapidly moved vertically into or out of the hot gas stream. In the heating portion of the test cycle the vane leading edge at the hot zone center line (see fig. 1) reached the desired test temperature within 30 seconds. In the cooling portion of the test cycle the vane leading edge cooled to black heat within 30 seconds and to approximately 150° C in 3 minutes. Optical pyrometer temperature measurements of vane areas other than the leading edge at the hot zone centerline showed that appreciable temperature gradients existed during vane exposures. For example, for NC-350 reaction sintered Si_3N_4, the leading edge temperature decline 1.6 cm above and below the hot zone centerline was about 100° C. Also, for NC-350, the temperature decline 1.2 cm back from the leading edge along the hot zone centerline (on the vane major flat surface) was about 140° C. The maximum heat transfer coefficients at the vane leading edge tip for heating and cooling were estimated to be 6200 and 1100 W/m2-°C, respectively.

Inspection. - Dense specimens were inspected in the as-received condition under black light after treatment with a penetrating oil, an emulsifier, and a powder developer. After this inspection, all dense specimens were degreased, dried in an oven at 150° C, weighed to + or - 0.2 mg and individually packaged for storage until use. As-received porous specimens were examined with a ×30 binocular microscope, dried, weighed and individually packaged.

Each test vane was removed from the burner rig after 5, 50, and 125 cumulative cycles for inspection. Inspection consisted of weighing, fluorescent penetrant examination, ×30 binocular inspection, and photographing. These steps were also performed after reaching the 250 cycle exposure goal.

RESULTS AND DISCUSSION

The behavior of the ceramic vanes will be discussed in the order of the material categories listed in table I. The results consist of weight change measurements, photographs illustrating surface changes, and observations on thermal cycles to failure (separation of the vane into two pieces). Vane failures occurred close to the hot zone centerline (see fig. 1). With three exceptions, vanes that failed did so after completing at least one cycle involving heat-up, hold at test temperature, and still air cool down. A summary of specific weight changes and thermal cycles to failure is given in table V.

Thermal fatigue failures of vanes result from the growth of cracks which may originate at some leading edge surface imperfection or from some sub-surface flaw. For cyclic burner rig exposure, transient thermal stresses at the vane leading edge are compressive during vane heating and tensile during vane cooling. Transient thermal stresses in the vane interior and back from the leading edge in thicker sections are tensile during vane heating and compressive during vane cooling. Since ceramics are weaker in tension than in compression, cracks usually develop when tensile stresses act on surface imperfections or subsurface flaws. Thus, leading edge surface cracks would have the greatest tendency to grow during the cooling portion of a thermal cycle, while subsurface cracks would have the greatest tendency to grow during the heating portion of a thermal cycle. Sudden failure during heating can then be viewed as the rapid growth of an internal crack or cracks, while sudden failure during cooling can be viewed as the rapid growth of a leading edge surface crack or near-surface crack. Internal and surface cracks could also merge to cause sudden fracture of a vane. In this work, vane thermal fatigue failures during heating and during cooling were both encountered.

NC-132 Hot Pressed Si_3N_4

As shown in table V, the weight changes for the six NC-132 vanes tested at 1260°, 1315°, and 1370° C were relatively slight with all vanes surviving 250 cycle exposures. No cracks were found in the vanes by fluorescent penetrant inspection. A plot of weight change versus exposure

duration for the two batches of NC-132 HP Si_3N_4 vanes is presented in figure 5. Batch 2 vanes displayed a more uniform weight change behavior with respect to exposure duration and exhibited less weight change than the Batch 1 vanes. As figure 5 shows, end-point weight loss increased with increasing test temperature. This correlates with the appearance of the vanes which exhibited increased oxide loss for increased exposure temperatures. The only oxide found by X-ray diffraction on NC-132 hot zone leading edges was alpha cristobalite (silica). Figure 6 illustrates the oxide loss-temperature relationship for the Batch 1 vanes. Loss of oxide was not evident at 1260° C, apparent at 1315° C, and very pronounced at 1370° C.

The weight losses reflected in figure 5 contast with the parabolic oxidation weight gain behavior for NC-132 observed in a static oxidizing environment (ref. 9). The losses in the high velocity oxidizing gas stream most likely reflect erosive action on a viscous silica surface layer. The viscosity of the silica layer formed during the oxidation of hot pressed Si_3N_4 is likely reduced by Mg (intentionally added as MgO) and the commonly present impurity elements Ca, Al, Fe, Na, K, and Mn which tend to concentrate in the silica scale formed (ref. 10). Undetected very fine cracks may also be present in the silica surface layers of cyclically oxidized hot pressed Si_3N_4 which may promote spalling. The cracks can result from the transformation of beta-cristobalite to alpha-cristobalite on cooling through the temperature range 270° to 200° C with an accompanying 1 percent decrease in volume (ref. 11). Cracks could also result from tensile stresses arising from a SiO_2/Si_3N_4 thermal expansion mismatch (ref. 11).

In the 1370° C tests it was observed that, although the Batch 1 NC-132 vane lost more weight than did the Batch 2 NC-132 vane for the total test duration, at first, more oxide formed on the Batch 1 vane than on the Batch 2 vane. This condition was most pronounced after 50 cycles (10 hr) of exposure and is illustrated in figure 7. The reasons for the differences in oxidation behavior of the two batches of NC-132 vanes may be related to some critical differences in impurity levels in the two batches. However, the AFML spectrographic analyses for the two batches of NC-132 given in table II show the level of total metallic impurities to be very

similar. Perhaps a small difference in Mg content between the two NC-132 batches may be responsible. This supposition is based on the results of Cubicciotti, et al. (ref. 9) who have concluded that the rate of oxidation of NC-132 hot pressed Si_3N_4 is controlled by the rate of diffusion of Mg out of the NC-132 body. Further AFML characterization of the NC-132 batches may help to explain the differences in oxidation behavior observed.

NC-350 And KBI Reaction Sintered Si_3N_4

Seven of the nine NC-350 vanes survived 250 cycle exposures as indicated by the final weight change entries in table V for exposure temperature of 1260° , 1315° , and 1370° C. No cracks were found by binocular inspection at ×30. The failure of the Batch 2 NC-350 vane after 20 cycles at 1260° C was due to installation damage. Only the Batch 1 NC-350 vane tested at 1315° C failed in thermal fatigue, with this failure occurring after approximately 76 cycles. No cracks were found at the 50 cycle inspection point. It is not known at what point in the 76th cycle this vane failed. In contrast, only one out of nine KBI vanes survived a 250-cycle exposure; this exposure was at 1260° C for a Batch 1 vane. A Batch 2 KBI vane tested at 1260° C for five cycles was found to have a hot zone transverse leading edge crack and was not tested further. A Batch 3 KBI vane failed during 6th cycle heat up after having completed five cycles at 1260° C with no cracking observed at that point. Testing at 1315° C was totally unsuccessful for KBI vanes-two vanes failed during first cycle cooling. These failures were probably due to as-received leading edge surface imperfections or near-surface imperfection of sufficient severity to cause fracture under the tensile stresses generated during cooling. The third KBI vane tested at 1315° C failed during first cycle heating, probably due to a subsurface flaw acted on by internal tensile stresses generated during heating. Because of the early KBI vane failures at 1315° C, additional tests were performed at 1205° C instead of 1370° C as originally planned. Even at 1205° C, the 3 KBI vanes tested displayed only limited lives, failing during heating after completing 98, 20 and 5

cycles. The failures are attributed to subsurface flaws. No cracks had been noted in inspections prior to the failures. At this point it is well to recall previously stated characterization remarks (Specimens and Apparatus Section) comparing the KBI RS Si_3N_4 to the NC-350 RS Si_3N_4; the KBI vanes had:

a. nonuniform, rough ground surfaces
b. higher variability in density and open porosity within vanes and batch to batch
c. areas of high porosity
d. larger pores

It is worthy of note that the single 250-cycle surviving KBI vane had the lowest open porosity of 8.2 percent. The range of open porosity for the 8 KBI vanes that failed was 13.5 to 20.9 percent.

The final weight changes for the RS Si_3N_4 materials given in table V indicate a considerable variability in weight change behavior within batches (NC-350 at 1260° and 1370° C) and between NC-350 and KBI at 1260° C. For both types of RS Si_3N_4, high weight gains correlated with high open porosity percentages - this observation will be discussed further. For all RS Si_3N_4 vanes tested for 250 cycles, alpha cristobalite was found by surface X-ray diffraction. This was the only oxidation product detected. Any differences in starting alpha/beta ratios for the RS Si_3N_4 vanes were not reflected in the oxidation results to be discussed.

A plot of specific weight change versus exposure duration at 1260° C is presented in figure 8 for three RS Si_3N_4 vanes exposed for 250 cycles (50 hr) - two of NC-350 and one of KBI material. Also plotted are two 5 cycle data points for the other 2 KBI vanes tested. The data for the third NC-350 vane which failed after 20 cycles is excluded because of vane weight uncertainty related to installation damage. The percent of theoretical density and the percent open porosity for each vane previously given in table IV are also included in the figure. The Batch 1 KBI vane was chipped on removal from the burner rig after the first exposure of five cycles. Therefore, the entire curve for this vane is lower than the true curve, but the shape of the curve does show the weight change versus time relationship. The reason for the five cycle weight loss for the

Batch 1 NC-350 vane is unexplained. There was no chipping damage noted on the vane. For exposure durations past 50 cycles (10 hr) the forms of the three curves in figure 8 are similar, and show decreasing rates of oxidation. This weight change behavior is similar to the second stage of oxidation observed by Davidge and co-workers (ref. 11) for the 1200° and 1400° C static air oxidation of RS Si_3N_4 after an initial very short (less than 15 min) first stage of rapid weight gain. Their material had the high open porosity of 21 percent and was more subject to internal oxidation than were the three vanes of figure 8 which had much lower open porosity percentages of 8.2 (KBI Batch 1), 11.1 (NC-350 Batch 3), and 7.8 (NC-350 Batch 1). We did observe initial high weight gains at five cycles (1 hr), as plotted in figure 8, for two KBI vanes with open porosities of 18.1 and 20.9 percent. Our three vanes of lower open porosities did not display the initial rapid weight gain but did display the second stage behavior described by Davidge and co-workers. This stage was characterized by the formation of a protective oxide layer which blocks pores and prevents deep internal oxidation. The very slow oxidation rate for the NC-350 Batch 1 vane (7.8 percent open porosity) in comparison to the NC-350 Batch 3 vane (11.1 percent open porosity) is believed due to the differences in open porosity. The reason for the differences in oxidation behavior for the NC-350 Batch 1 vane and the KBI Batch 1 vane which had very similar open porosities (7.8 percent vs 8.2 percent) may be related to impurity levels or to the size and distribution of pores. Reference to table II shows that the NC-350 material has 0.45 percent metallic impurities in comparison to 0.73 percent metallic impurities for the KBI material. AFML has determined the X-radiographic and microstructural characteristics of NC-350 and KBI RS Si_3N_4 materials and reports that the KBI material has larger pores, less well distributed porosity, and more pronounced sample to sample density and microstructural nonuniformity than the NC-350 material (ref. 7).

From the above discussion on the oxidation of RS Si_3N_4 it is clear that open porosity is an important variable in the high gas velocity cyclic oxidation behavior of the material. Warburton and co-workers (ref. 12) have noted that in the oxidation of RS Si_3N_4 the sealing of the surface was faster and occurred at a lower weight gain as the density of the material

increased due to the reductions in the number and size of pores. They suggest that the pore structures influencing oxidation behavior in RS Si_3N_4 can be very different depending upon the techniques used in the preparation of the green silicon compact. Based on the AFML characterizations of the NC-350 and KBI RS Si_3N_4 materials and our pretest inspection of the vanes, the oxidation results and the vane failures discussed earlier correlate with the percentage of open porosity, the structural uniformity, and the surface condition of the two types of RS Si_3N_4. The NC-350 material was superior by virtue of lower open porosity, and good structural uniformity and machined surface condition. The KBI RS Si_3N_4 vanes that failed during the first cycle probably did so because of flaws present in the vanes in the as-received condition. The KBI RS Si_3N_4 vanes that failed during cyclic thermal exposure likely did so as a result of the growth of cracks from preexisting flaws or from cyclic oxidation induced damage. Reduced strengths in statically oxidized RS Si_3N_4 cooled below 200° C have been reported by Davidge and co-workers as a result of severe cracking of the silica layer due to thermal expansion mismatch augmented by the beta-cristobalite to alpha-cristobalite transformation (ref. 11). They reason that surface cracks in the alpha-cristobalite pass into the RS Si_3N_4 and connect with subsurface pores whose walls may be lined with cracked silica. This type of damage would be augmented by cycling above and below the cristobalite transformation as in our work.

Three vanes of NC-350, each representing a different RS Si_3N_4 batch were successfully tested for 250 cycles (50 hr) at 1370° C. Photographs of these three vanes are shown in figure 9 and plots of specific weight change versus time are presented in figure 10. Figure 9 shows that the general post-test appearance of the vanes from the three different batches is very similar as well as the hot zone leading edges shown at ×10. The white stripes present on the Batch 2 NC-350 vane in the as-received condition (fig. 2) are still present after testing. The vane as a whole is lighter in color as a result of the oxidation exposure, but the stripes do not appear to have had any visual effect on the nature of the oxidation. Figure 10 shows that all three NC-350 vanes lost weight as a result of the first five cycles of exposure. At 1370° C the reason for

these losses is unexplained. The vanes had been oven dried before initial weighing. Beyond five cycles the vanes continuously gained weight at slow rates. Vanes from Batches 2 and 3 with similar starting open porosities of 16.3 and 14.0 percent, respectively showed very similar weight change behavior. The vane from Batch 1 with the lower open porosity of 8.3 percent showed the least total weight gain after the first five cycles and oxidized at the slowest rate. This reflects the benefit of low open porosity so that in a high temperature oxidizing environment, rapid oxide sealing of the RS Si_3N_4 surface occurs with minimal damaging internal oxidation.

NC-435 Siliconized SiC

Final weight changes and cycles completed before failure for the nine NC-435 vanes tested are given in table V. Only four of the NC-435 vanes completed 250 exposure cycles. No cracks were found at the 250 cycle inspections by fluorescent penetrant examination. However, in one instance, the remnant of an apparently healed longitudinal crack in the hot zone leading edge of a Batch 2 vane exposed at 1315° C for 250 cycles was found in binocular examination. This longitudinal crack, and two transverse cracks also in the vane leading edge, had been found by fluorescent penetrant inspection after 125 cycle exposure. With the binocular microscope, several tiny metallic beads were noted lined up along the longitudinal crack. This lengthwise crack may relate to line flaws parallel to the vane axis detected in pretest radiographic inspection by AFML (ref. 8). The other two vanes of Batch 2 NC-435 also survived 250 cycle exposures at 1205° and 1260° C as did a vane of Batch 1 exposed at 1205° C. There was no evidence of cracking for these three vanes. The superior behavior of the Batch 2 NC-435 vanes over Batches 1 and 3 vanes was also noted for Batch 2 material in room temperature and 1200° C flexural strength by Larsen and Walther at IITRI (ref. 7). They pointed out that by qualitative X-ray diffraction analysis, Batch 2 had the least free silicon. The apparent importance of free silicon on the burner rig oxidation and thermal fatigue behavior of NC-435 SiC will be discussed. For all NC-435 vanes tested for 250 cycles, alpha cristobalite was the only oxidation product detected by surface X-ray diffraction.

Two NC-435 vanes being tested at 1260° C failed on heat-up for the 135th cycle (Batch 1) and the 126th cycle (Batch 3). As discussed previously, vane failures occurring during heat up suggest that internal tensile stresses have acted on a thermal fatigue crack to propagate the crack to failure. Two other NC-435 vanes, both from Batch 3, one being tested at 1205° C and one starting testing at 1260° C, failed during cooling in the 126th cycle and the first cycle, respectively. The first cycle cooling failure with the vane leading edge in tension was likely due to a vane surface imperfection present in the as-received condition. The one NC-435 vane tested at 1370° C failed in approximately 19 cycles; the point in the cycle when failure occurred was not noted.

A plot of specific weight change versus exposure duration at 1205° C for three NC-435 vanes is presented in figure 11, and photos of the vanes are shown in figure 12. The weight change behavior at 1205° C was similar for the vanes representing three different batches of material. There was some indication that the Batch 3 vane was beginning to gain weight at a greater rate in the 50 to 125 cycle exposure interval, but then it failed during 126th cycle cooling. The curve for the Batch 1 vane which survived 250 cycles is extrapolated past 125 cycles because a chip in the base of the vane precluded an accurate final weight determination. In the 1205° C testing (and in tests at higher temperatures to be discussed) it was noted that buildups of tiny metallic bead-like particles and glassy oxide took place as illustrated in figure 12. These buildups were most prevalent for Batch 3 NC-435 and least prevalent for Batch 2 NC-435. The Batch 3 vane was pieced together after failure so that the comparison could be made. X-ray diffraction analysis of the buildup material on the Batch 3 vane showed $FeSi_2$ and Si to be present. And spectrographic analysis on the buildup material showed that the scale material contained between 8 and 12 w/o iron and between 7 and 11 w/o aluminum. These analyses contrast with the 0.58 w/o metallic impurities (iron and aluminum, major) determined for a Batch 3 NC-435 material sample as given in table II. Although silicon melts at 1430° C, iron and aluminum form eutectics with silicon at 1208° and 577° C, respectively. We believe the failure of the Batch 3 vane was due to a flaw which developed during burner rig exposure as a result of a localized heavy exudation of a molten silicon-iron-aluminum eutectic.

We reason this flaw to be a partial void containing some silicate oxidation product which may well be cracked. Evidence for the heavy exudation of molten material can be seen in figure 13 which shows a front view and a side view of the hot zone leading edge of the Batch 3 NC-435 vane. The front view shows a particularly heavy buildup noted at the 125 cycle inspection. The side view shows the pieced-together vane which failed at the heavy buildup during the 126th cycle cooling. Glassy oxide streaks and buildups can also be noted. Figure 13(a) can likewise be compared with figure 12(b) for noting the coincidence of the failure point and the heavy buildup. We suggest that the Batch 3 NC-435 vane had high near-surface concentrations of silicon, iron, and aluminum resulting in eutectic formation and "sweating out" of the molten eutectic during burner rig exposure. Based on vane appearance in figure 12, such presumed deleterious near-surface concentrations of silicon, iron, and aluminum were considerably less for the Batch 1 NC-435 vane and very slight for the Batch 2 NC-435 vane. This batch ranking, 3-1-2, based upon degree of sweat-out differs from a batch ranking, 2-3-1, based upon highest to lowest concentration of metallic impurities (iron and aluminum, major), given in table II. Apparently, for the metallic impurity levels 0.68, 0.58, and 0.49 percent, chemical inhomogeneties within the vane can overide the effects of overall impurity level.

A plot of specific weight change versus exposure duration at 1260° C for three NC-435 vanes is presented in figure 14. Vanes from Batches 1 and 3 failed during heating for the 135th and 126th exposure cycle, respectively. Photos of the Batch 3 vane are given in figure 15. In contrast to the similar weight change behavior at 1205° C for vanes representing the three different NC-435 batches, batch differences were apparent in the 1260° C testing as shown in figure 14. The Batch 3 vane showed a more rapid weight gain than vanes of the other two batches. As was noted at 1205° C, the Batch 3 vane tested at 1260° C was again most prone to the development of the bead-like particle buildup that we feel results from silicon eutectic sweat-out previously discussed. Sweat-out was not as pronounced for the Batch 3 vane exposed at 1260° C as for the Batch 3 vane exposed at 1205° C. And there was no heavy buildup at the failure point of the vanes exposed at 1260° C as there was for the vane exposed

at 1205° C. The photos in figure 15 show the Batch 3 vane after 125 cycle exposure at 1260° C. In addition to the clusters of bead-like particles, there was a large collection of frothy oxide on the vane major flat surface which had been swept back from the leading edge by the Mach 1 hot gas stream.

At 1315° C only a Batch 2 NC-435 vane was tested, and it completed the planned 250 cycle exposure. As previously noted, a transverse crack and two longitudinal cracks found by fluorescent penetrant inspection after 125 cycles in this best batch vane healed during subsequent exposure. A plot of specific weight change versus exposure duration at 1315° C is presented in figure 16, and photos of the vane are shown in figure 17. For judging the effect of test temperature on the Batch 2 NC-435 vanes, weight change plots and photos for 1205° and 1260° C tests are included in figures 16 and 17 for comparison with the 1315° C results. Figure 16 shows that after 250 cycles at 1315° C NC-435 has begun to lose weight while at 1205° and 1260° C the material is still gaining weight. The weight loss behavior at the highest temperature, 1315° C, may be due to Mach 1 gas stream erosive action on a less viscous silica oxidation product. It did appear, as can be noted in figure 17, that less bead-like particle clusters remained on the 1315° C test vane than on the 1260° C test vane. There were no particle clusters at 1205° C. The appearance of the 1260° C vane in comparison to the 1205° C vane is regards to particle clusters would be consistent with an assumption that the amount of silicon eutectic bleed out responsible for the particle clusters would increase with increase in exposure temperature. The lesser number of particle clusters remaining on the 1315° C vane in comparison to the 1260° C vane may be due to increased spalling tendency or erosive action at the higher exposure temperature. Such actions on the particle clusters may explain the 1315° C weight loss behavior.

One NC-435 vane of Batch 1 material was tested at 1370° C; it failed after only 19 cycles. The bleed-out of silicon eutectic was very heavy as shown in the figure 18 photos of the front and side views of the leading edge. Failure occurred above the leading edge region shown. The figure 18(a) photo shows two fine transverse cracks in the leading edge. Longitudinal cracks just back of the leading edge can be seen in figure 18(b).

In figure 18(b) the heavy particle clusters back of the leading edge begin just down stream of the longitudinal cracks suggesting that the particle cluster material bled out along the length of the cracks and was swept back by the Mach 1 hot gas stream.

CONCLUDING REMARKS

In this investigation, four ceramic materials considered to have good potential for gas turbine usage were evaluated in a simulated vane shape for their resistance to oxidation-erosion and thermal fatigue experienced in a Mach 1 gas velocity burner rig simulating a turbine engine environment. The simulated vane shape incorporated a wedge-shaped leading edge, rapidly heated to temperatures between 1205° and 1370° C, causing the material to experience alternating thermal stresses during cyclic exposure. The exposure goal of 250 cycles was reached on 18 of the 33 vanes tested, and at least one vane of each of the four materials tested completed a 250 cycle test. Results of this study supplement physical property characterization work by Air Force Materials Laboratory and extensive mechanical and physical property determinations by IIT Research Institute under AFML contract.

Specific conclusions regarding each of the four materials tested in the Mach 1 gas velocity burner rig are as follows:

1. The Norton NC-132 hot pressed Si_3N_4 vanes were most resistant to thermal fatigue damage and to net oxidation weight changes.

2. Differences in the weight change-time behavior and in the end-point weight change for the two batches of NC-132 tested are thought to reflect the erosive action on silica oxidation products of somewhat different viscosity dependent on the amounts of impurity elements present in the NC-132 batches.

3. Percentage open porosity and pore size are very important features of reaction sintered Si_3N_4 which affect oxidation weight gain and resistance to thermal fatigue. Thus the Norton NC-350 material with less open porosity and smaller pores was apparently superior to the KBI material. However, the behavior of the two materials might have been more comparable if the KBI vanes had been fully diamond ground as

were the NC-350 vanes. More similar behavior might also have been observed if the NC-350 vanes had been tested in the standard thickness as were the KBI vanes. The thermal stresses generated in the thinner NC-350 vanes during heating and cooling were probably somewhat lower than the stresses generated in the KBI vanes.

4. The amount of free silicon, the distribution of the free silicon, and the concentrations of impurity elements iron and aluminum determined the degree of exudation of a molten silicon eutectic from Norton NC-435 siliconized SiC during high temperature exposure. This molten exudation can be the source of flaws leading to thermal fatigue failure.

REFERENCES

1. Wade, T. B.: Property Screening and Evaluation of Ceramic Vane Materials. IITRI-D6114-I6, IIT Research Institute, 1976.

2. Sanders, William A.; and Probst, Hubert B.: Evaluation of Oxidation Resistant Nonmetallic Materials at 1204° C (2200° F) in a Mach 1 Burner. NASA TN D-6890, 1972.

3. Sanders, William A.; and Probst, Hubert B.: High Gas Velocity Burner Tests on Silicon Carbide and Silicon Nitride at 1200° C. NASA TM X-71479, 1973.

4. McLean, Arthur F.; and Baker, Robert R.: Brittle Materials Design, High Temperature Gas Turbine. IR-10, Ford Motor Company, 1976. (AMMRC CTR 76-31, AD-B015331.)

5. de Biasi, Victor: Ford Runs Uncooled Ceramic Turbine Engine at 2500° F. Gas Turbine World, vol. 7, no. 3, June-July 1977, pp. 12-18.

6. Bratton, Raymond J.; and Miller, Donald G.: Brittle Materials Design, High Temperature Gas Turbine, Vol. 1. Final Rep. 1 July 1971-30 June 1976, Westinghouse Electric Corp., 1976. (AMMRC 76-32, Vol. 1, AD-A045104.)

7. Larsen, D. C.; and Walther, G. C.: Property Screening and Evaluation of Ceramic Vane Materials. IITRI-D6114-ITR-24, IIT Research Institute, 1977.

8. Wade, T. B.: Property Screening and Evaluation of Ceramic Vane Materials. IITRI-D6114-I12, ITT Research Institute, 1976.

9. Cubicciotti, D. D.; Jones, R. L.; and Lau, K. H.: High Temperature Oxidation and Mechanical Properties of Silicon Nitride. SRI-5522-1, SRI International, 1977.

10. Singhal, S. C.: Thermodynamics and Kinetics of Oxidation of Hot-Pressed Silicon Nitride. J. Mater. Sci., vol. 11, Mar. 1976, pp. 500-509.

11. Davidge, R. W.; et. al.: Oxidation of Reaction-Sintered Silicon Nitride and Effects on Strength. Special Ceramics 5, P. Popper, ed., British Ceramic Research Assoc. 1972, pp. 329-343.

12. Warburton, J. B.; Antill, J. E.; and Hawes, R. W. M.: Oxidation of Thin Sheet Reaction-Sintered Silicon Nitride. J. Am. Ceram. Soc., vol. 61, no. 1-2, Jan.-Feb. 1978, pp. 67-72.

TABLE I. - CERAMIC VANE MATERIALS

Material	Number of batches	Vanes/Batch	Total vanes
NC-132 HP Si_3N_4	2	3	6
NC-350 RS Si_3N_4	3	3	9
KBI RS Si_3N_4	3	3	9
NC-435 RS SiC	3	3	9
			33

TABLE II. - SPECTROGRAPHIC ANALYSES FOR CERAMIC VANE MATERIALS (REF. 7)

Material	Total metallic impurities, w/o[a]					
	Batch 1	Batch 2	Batch 3	Average	Major	Oxygen[b], w/o (avg.)
NC-132 HP Si_3N_4	3.15	3.08		3.12	W, Mg, Fe, Al	3.33
NC-350 RS Si_3N_4	0.45	0.54	0.46	0.48	Fe, Al	0.84
KBI RS Si_3N_4	0.73	0.68	0.64	0.68	Fe, Al	c
NC-435 RS SiC	0.49	0.68	0.58	0.58	Fe, Al	0.34

[a]Spectrographic analysis.
[b]Neutron activation analysis.
[c]Not determined.

TABLE III. - X-RAY DIFFRACTION ANALYSIS FOR CERAMIC VANE MATERIALS (REF. 7)

Material	Phases present
NC-132 HP Si_3N_4	β-Si_3N_4 (major) + Si_2ON_2 (minor)
NC-350 RS Si_3N_4	α-Si_3N_4 (major) + β-Si_3N_4 (minor)
KBI RS Si_3N_4	β-Si_3N_4 + α-Si_3N_4 (equal amounts)
NC-435 RS SiC	α-SiC (major) + Si (minor)

TABLE IV. - DENSITY, OPEN POROSITY, AND α/β RATIO FOR REACTION SINTERED Si_3N_4 VANES

Material	Percent theoretical density[a]			Percent open porosity[a]			α/β weight ratio[b]		
	Vane number								
	1	2	3	1	2	3	1	2	3
NC-350 - Batch 1	80.3	80.1	80.6	7.8	8.9	8.3	7.13	6.56	6.05
- Batch 2	75.8	76.3	75.4	15.6	14.6	16.3	6.18	5.83	7.93
- Batch 3	79.8	76.9	79.0	11.1	17.1	14.0	3.63	3.81	3.23
KBI - Batch 1	83.8	80.7	80.8	8.2	13.5	13.9	(c)	(c)	1.32
- Batch 2	74.0	74.8	74.6	20.9	20.8	20.7	(c)	(c)	1.92
- Batch 3	76.0	77.4	75.9	18.1	15.4	18.7	(c)	(c)	3.57

[a]Based on values reported in reference 8 assuming a theoretical density of 3.2 g/cm^3.

[b]Determined at Lewis from surface X-ray diffractometer data, discounting the presence of amorphous phases, and assuming the possible presence of only the crystalline phases α-Si_3N_4, β-Si_3N_4 and Si. Si was not detected in any analysis.

[c]Not determined.

TABLE V. - SUMMARY OF 250 CYCLE SPECIFIC WEIGHT CHANGES OR CYCLES TO FAILURE FOR Si_3N_4 AND SiC VANES EXPOSED IN MACH 1 BURNER RIG

Material	Batch	Specific weight change[a] (mg/cm^2) after 250 cycles or cycles completed before failure			
		Vane leading edge temperature, ^oC			
		1205	1260	1315	1370
NC-132 HP Si_3N_4	1		-0.09	-0.28	-0.53
	2		+.04	-.18	-.23
NC-350 RS Si_3N_4	1		-1.11	~76 cycles	-.26
	2		[b]20 cycles	+2.99	+2 51
	3		+3.19	Completed 250 cycles (chipped)	+.73
KBI RS Si_3N_4	1	98 cycles/	+5.56	0 cycle\	
	2	20 cycles/	[c]5 cycles	0 cycle\	
	3	5 cycles/	5 cycles/	0 cycle/	
NC-435 Sil. SiC	1	+0.28	134 cycles/		~19 cycles
	2	+.35	+0.27	+.15	
	3	125 cycles\	1 cycle\, 125 cycles/		

[a]Based on affected area of 30 cm^2 or 29 cm^2 (NC-350).

[b]Installation-related failure.

[c]Crack in leading edge.

/ Failure during heat up.

\ Failure during cool down.

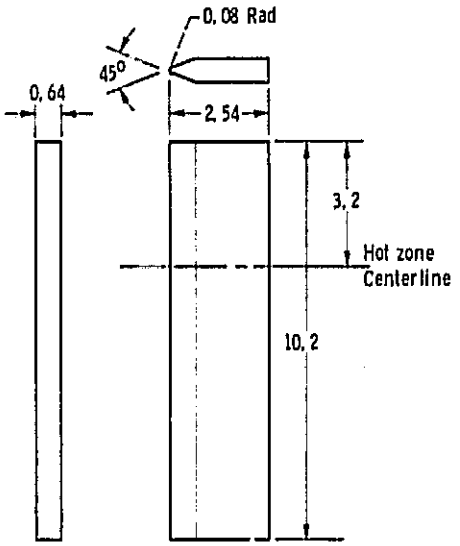

Figure 1. - Vane specimen for Mach 1 burner rig oxidation and thermal fatigue tests. (Dimensions are in cm.)

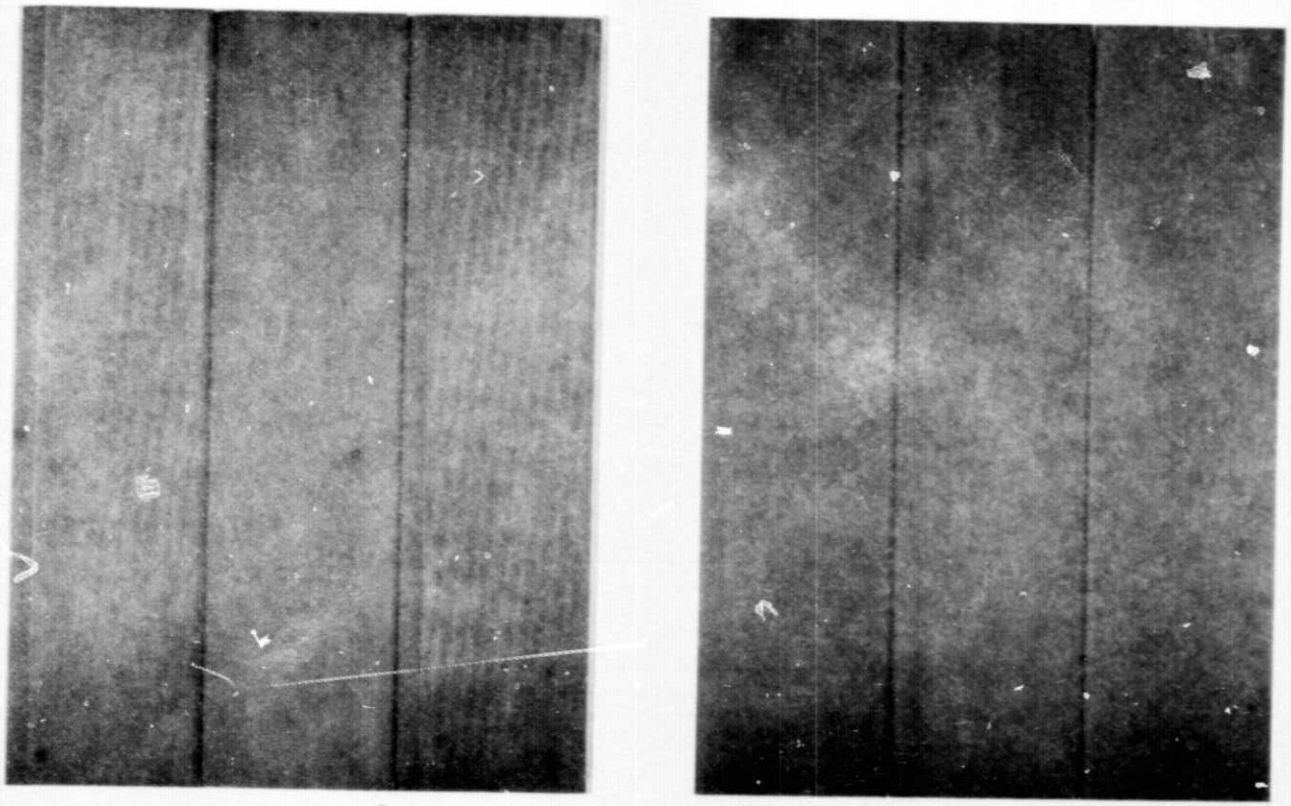

	Batch 2			Batch 3		
Vane No.	1	2	3	1	2	3
% Theo. density	75.8	76.3	75.4	79.8	76.9	79.0
% Open porosity	15.6	14.6	16.3	11.1	17.1	14.0

Figure 2. - Norton NC-350 reaction sintered Si_3N_4 vanes in as-received condition, X1.

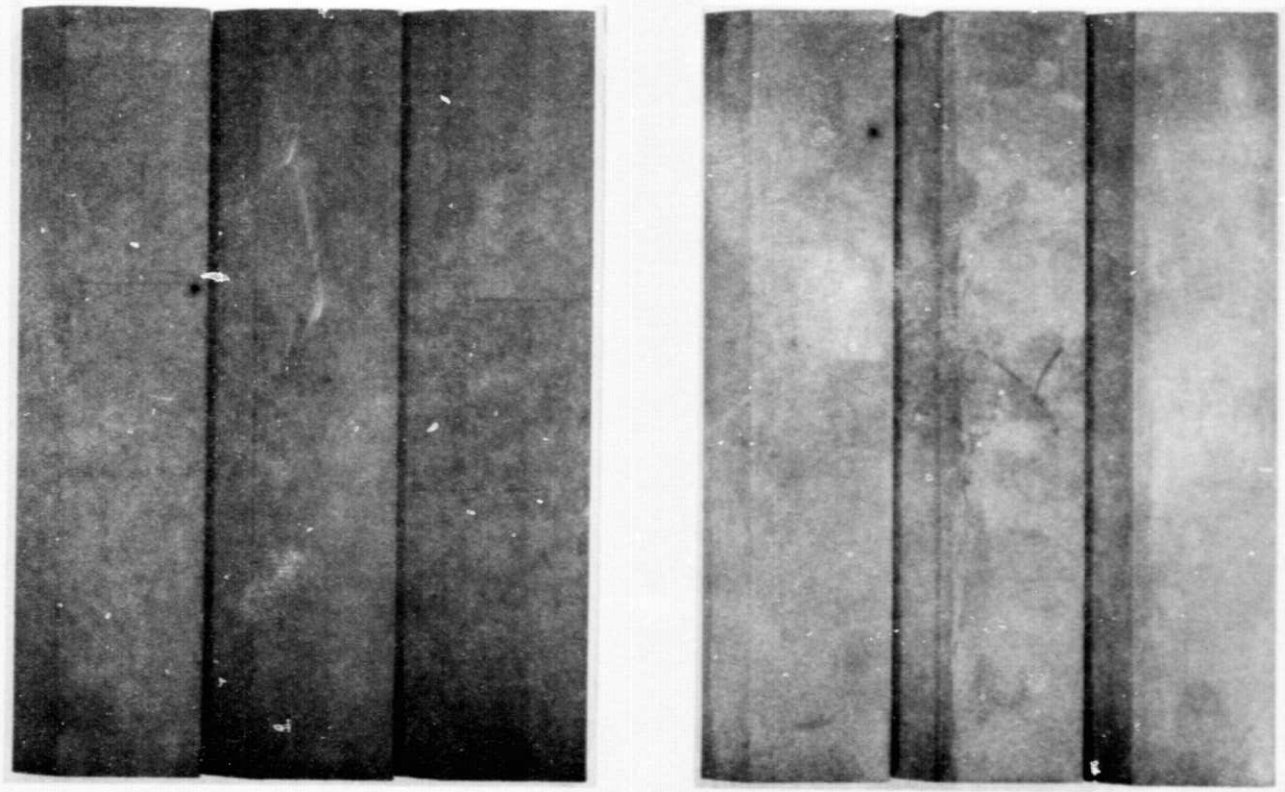

Batch 1 Batch 3

Vane No.	1	2	3	1	2	3
% Theo. density	83.8	80.7	80.8	76.0	77.4	75.9
% Open porosity	8.2	13.5	13.9	18.1	15.4	18.7

Figure 3. - KBI reaction sintered Si_3N_4 vanes in as-received condition, X1.

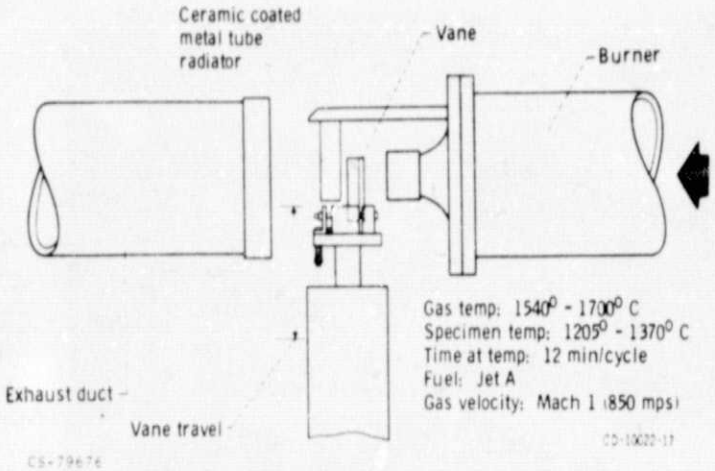

Figure 4. - Burner rig for simulated gas turbine environment.

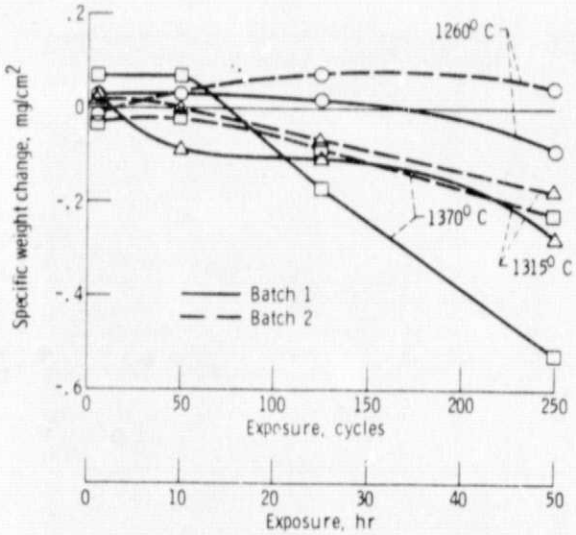

Figure 5. - Specific weight change for NC-132 HP Si_3N_4 vanes resulting from cyclic exposure in Mach 1 burner rig. Cycle: 12 minutes at test temperature, 3 minute still air cool.

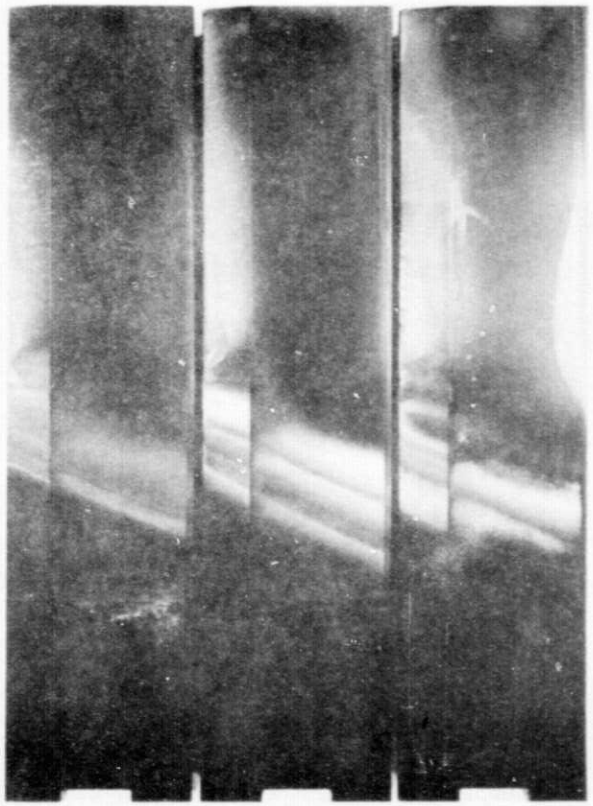

1260° C 1315° C 1370° C

(a) Side view, X1.

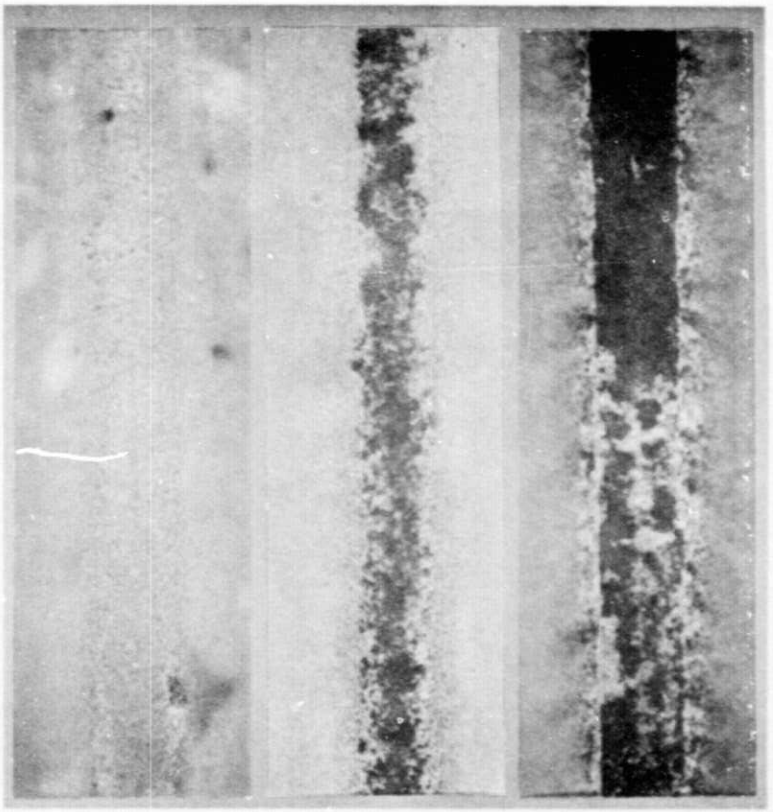

1260° C 1315° C 1370° C

(b) Front view, hot zone leading edges, X10.

Figure 6. - NC-132 Batch 1, HP Si_3N_4 vanes after 250 cycles exposure in Mach 1 burner rig. Cycle: 12 minutes at test temperature, 3 minute still air cool.

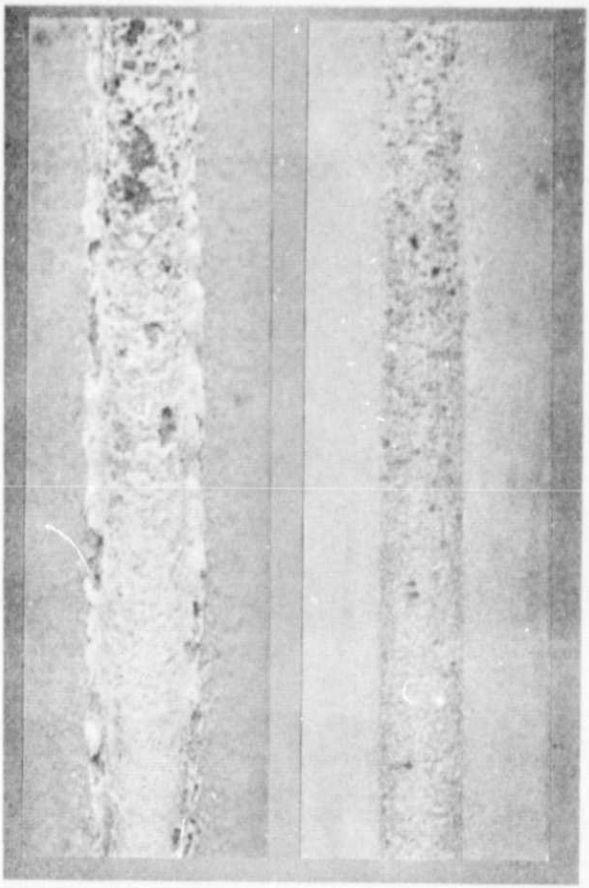

Batch 1 Batch 2

Front views

Figure 7. - NC-132 HP Si_3N_4 vane hot zone leading edges after 1370° C, 50 cycle exposure in Mach 1 burner rig. Cycle: 12 minutes at test temperature, 3 minute still air cool, X10.

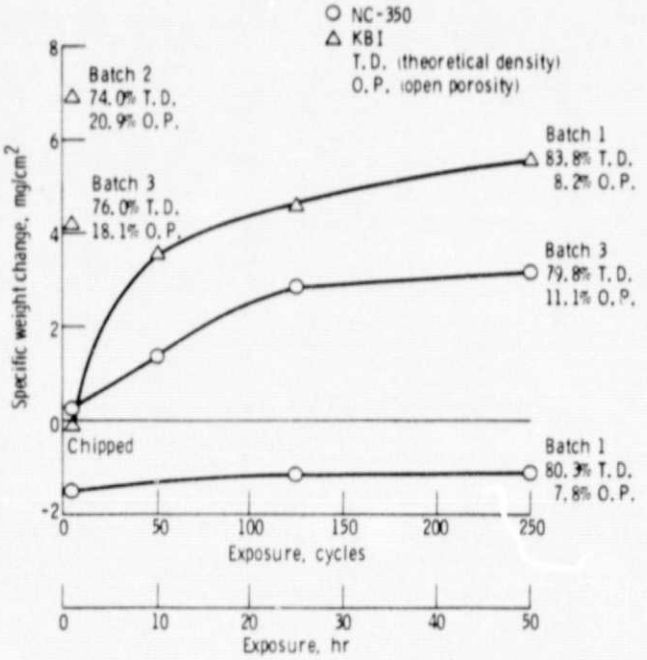

Figure 8. - Specific weight change for NC-350 and KBI R.S. Si_3N_4 vanes resulting from 1260° C cyclic exposure in Mach 1 burner rig. Cycle: 12 minutes at test temperature, 3 minute still air cool.

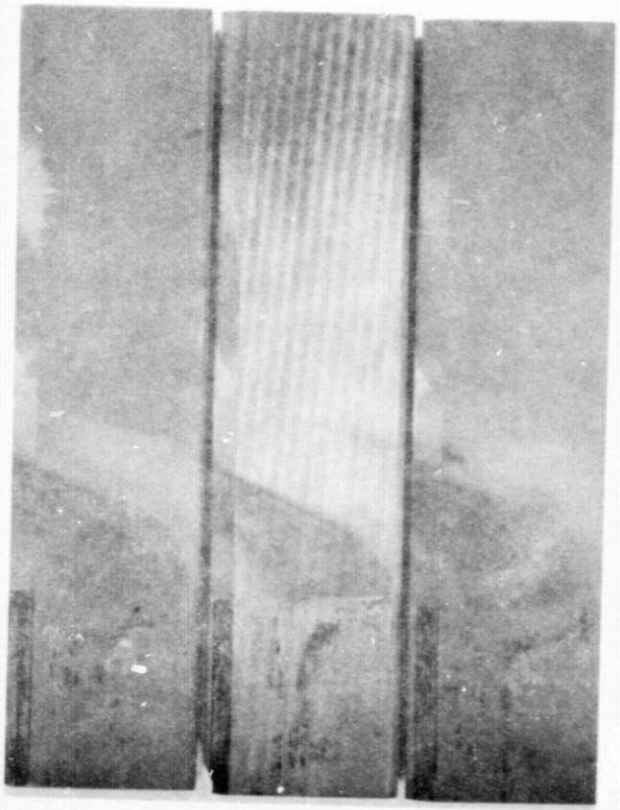

Batch 1 Batch 2 Batch 3

(a) Side views, X1.

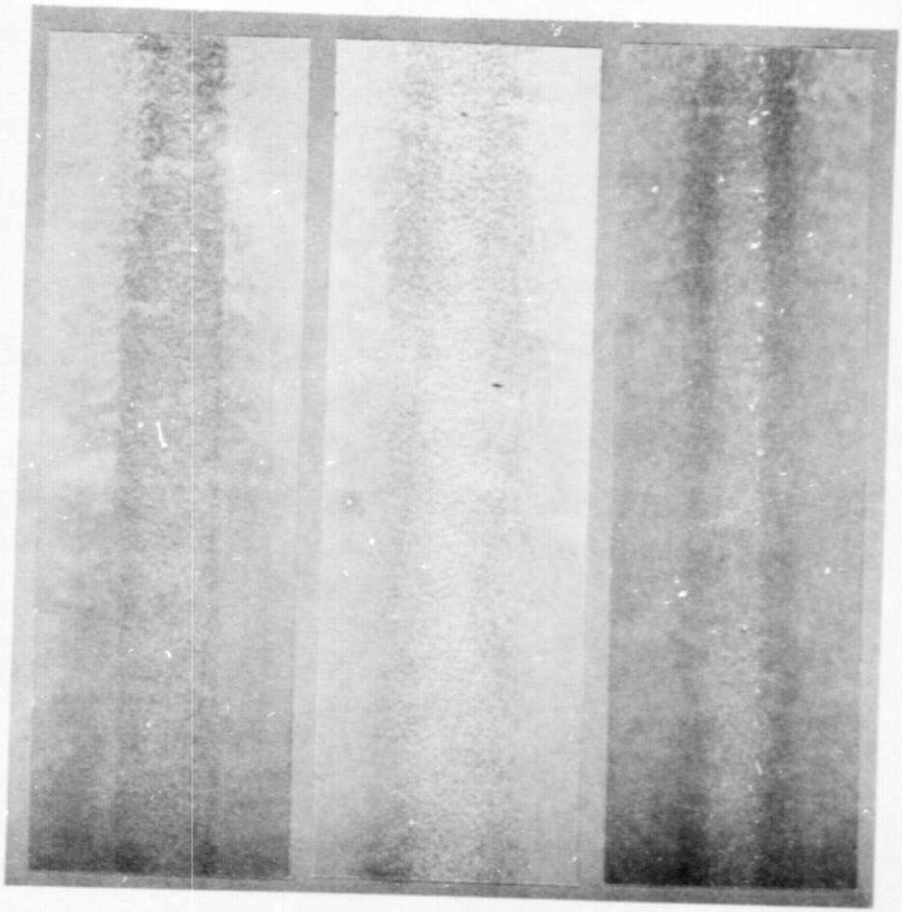

Batch 1 Batch 2 Batch 3

(b) Front view hot zone leading edges, X10.

Figure 9. - Norton NC-350 reaction sintered Si_3N_4 vanes after 250 cycle exposure in Mach 1 burner rig. Cycle: 12 minutes at 1370^0 C, 3 minute still air cool.

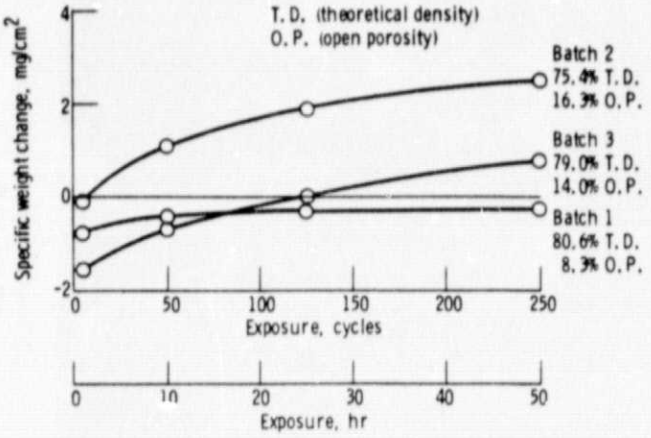

Figure 10. - Specific weight change for NC-350 R. S. Si_3N_4 vanes resulting from 1370° C cyclic exposure in Mach 1 burner rig. Cycle: 12 minutes at test temperature, 3 minute still air cool.

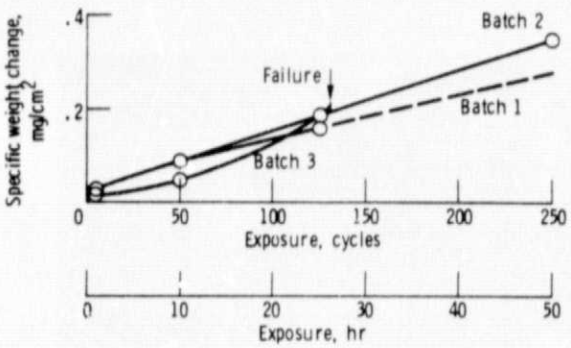

Figure 11. - Specific weight change for NC-435 siliconized SiC resulting from 1205° C cyclic exposure in Mach 1 burner rig. Cycle: 12 minutes at test temperature, 3 minute still air cool.

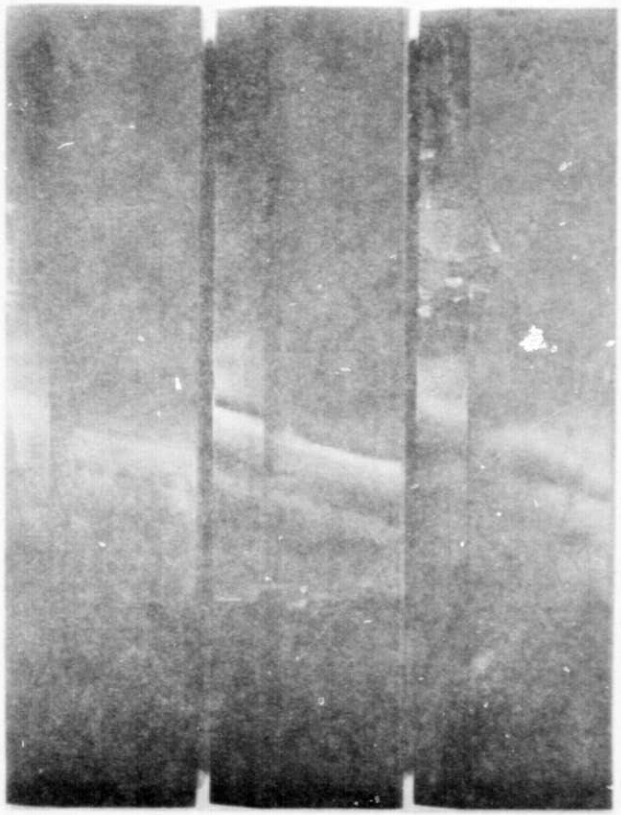

Batch 1 Batch 2 Batch 3
Cycles: 250 250 26

(a) Side view, X1.

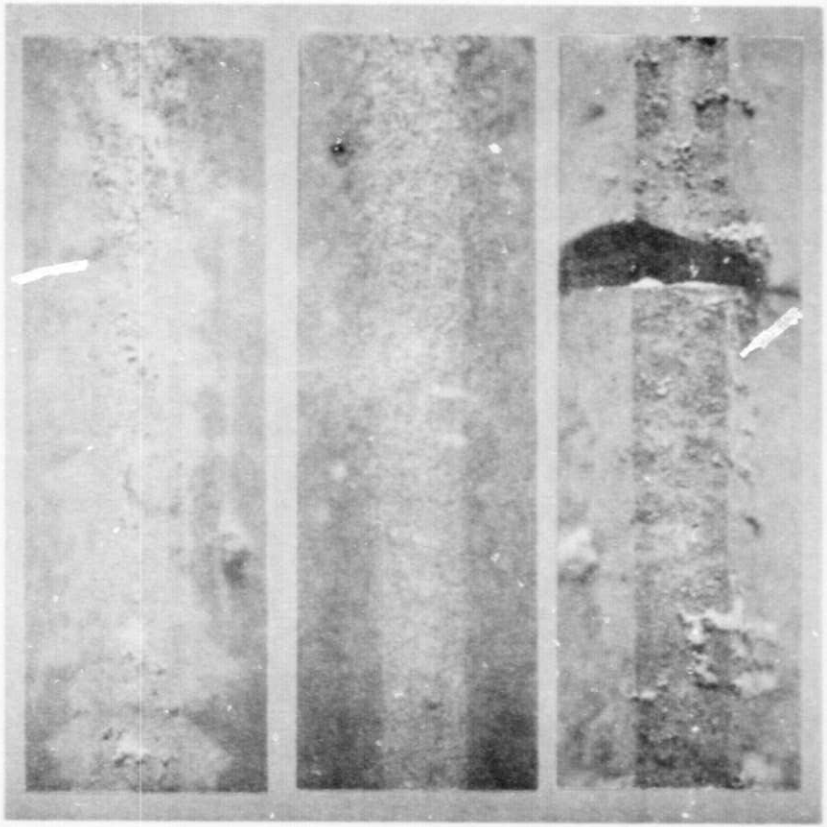

Batch 1 Batch 2 Batch 3

(b) Front view hot zone leading edges, X10.

Figure 12. - Norton NC-435 siliconized SiC vanes after exposure in Mach 1 burner rig. Cycle: 12 minutes at 1205^{0} C, 3 minute still air cool.

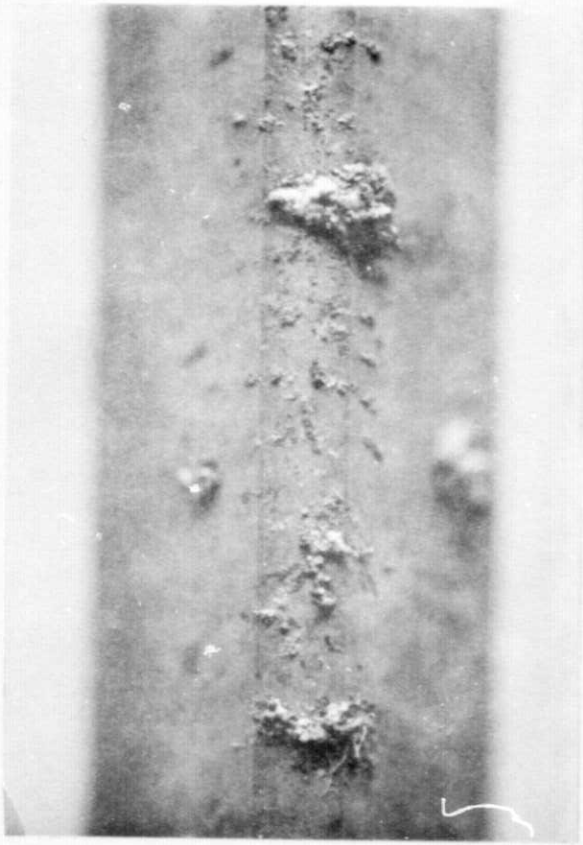

(a) Front view after 125 cycles.

(b) Side view after failure during 126th cycles. Cooling.

Figure 13. - Norton NC-435 siliconized SiC batch 3 vane hot zone leading edge after 1205° C exposure in Mach 1 burner rig. Cycle: 12 minutes at 1205° C, 3 minute still air cool. X10.

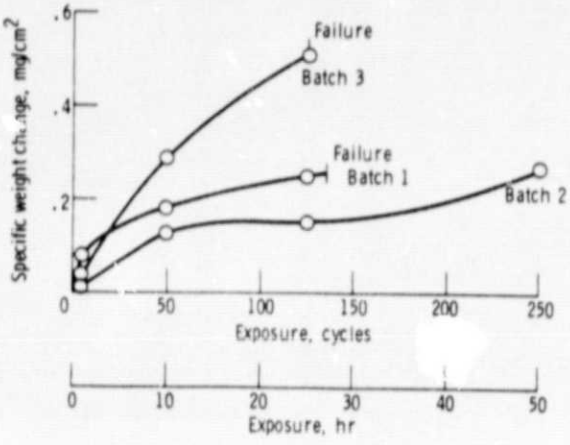

Figure 14. - Specific weight change for NC-435 siliconized SiC resulting from 1260° C cyclic exposure in Mach 1 burner rig. Cycle: 12 minutes at test temperature, 3 minute still air cool.

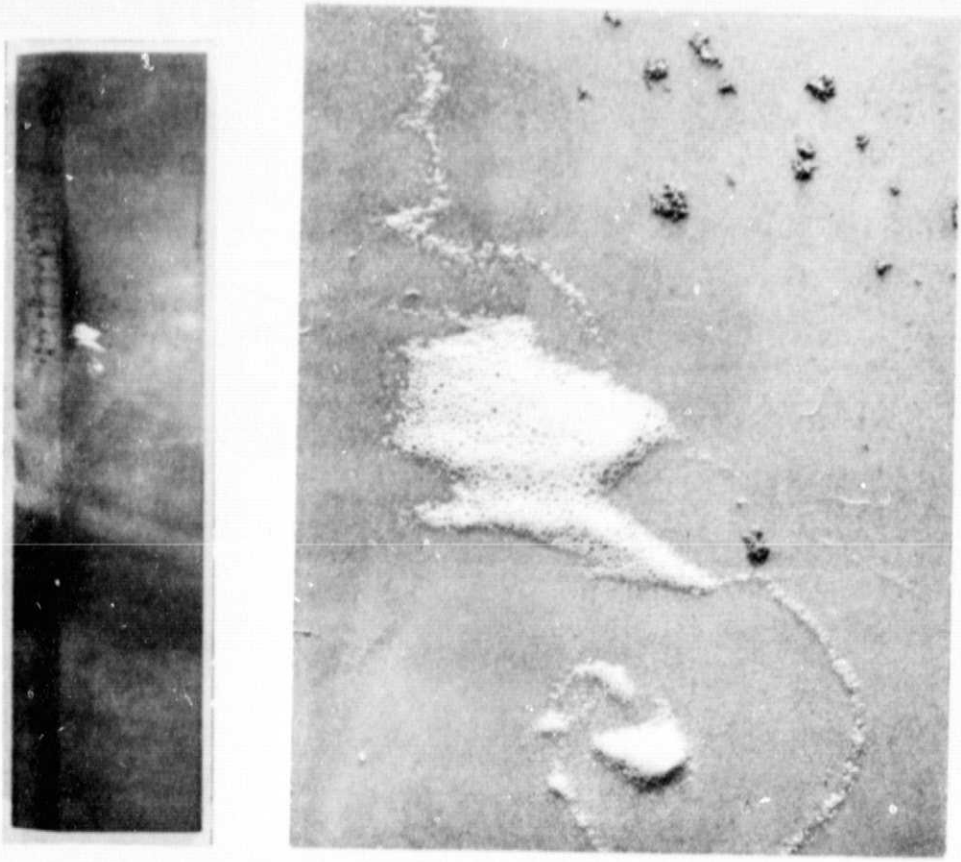

(a) Side view, X1.

(b) Side view, X10.

Figure 15. - Norton NC-435 siliconized SiC batch 3 vane after 1260^{0} C exposure for 125 cycles in Mach 1 burner rig. Cycle: 12 minutes at test temperature, 3 minutes still air cool.

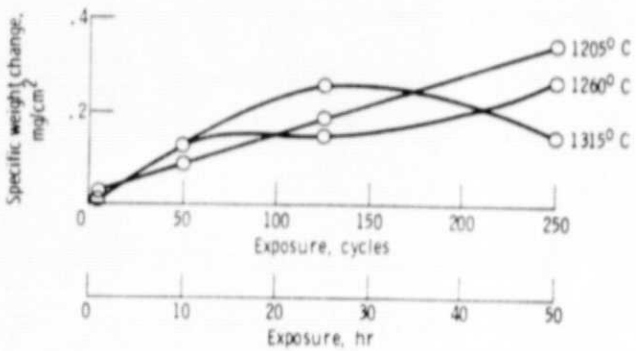

Figure 16. - Specific weight change for batch 2 NC-435 siliconized SiC resulting from cyclic exposure in Mach 1 burner rig. Cycle: 12 minutes at test temperature, 3 minute still air cool.

1205° C 1260° C 1315° C

(a) Side view, X1.

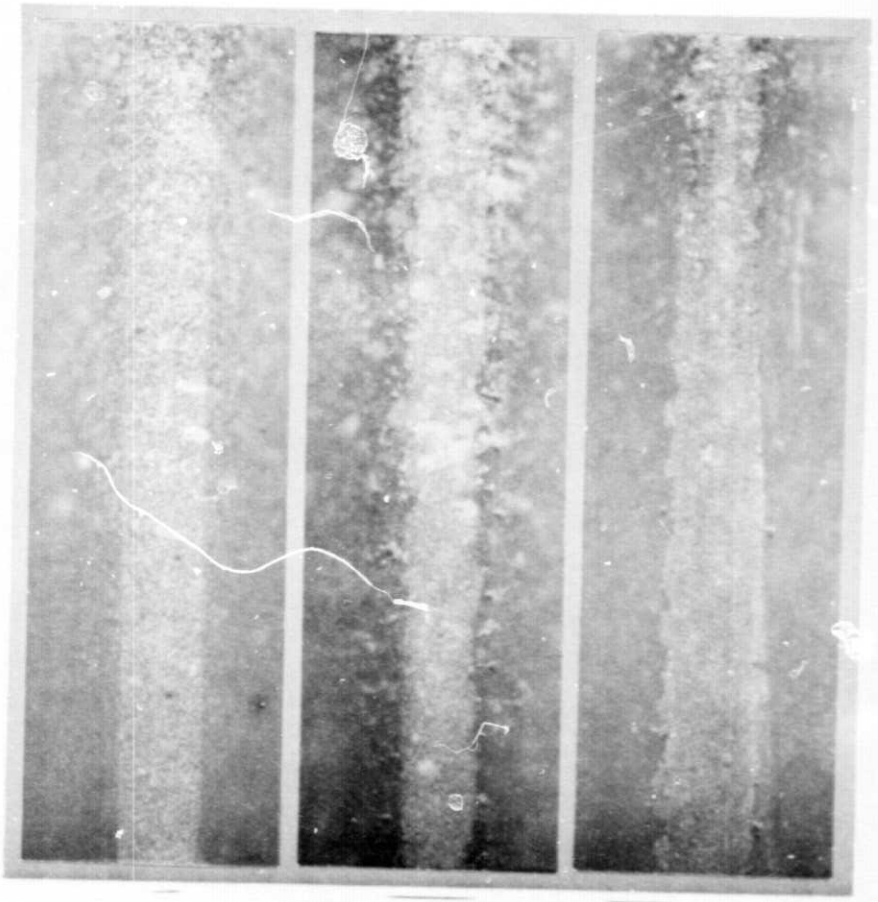

1205°C 1260° C 1315° C

(b) Front view hot zone leading edges, X10.

Figure 17. - Norton NC-435 siliconized SiC batch 2 vanes after 250 cycle exposure in Mach 1 burner rig. Cycle: 12 minutes at test temperature, 3 minute still air cool.

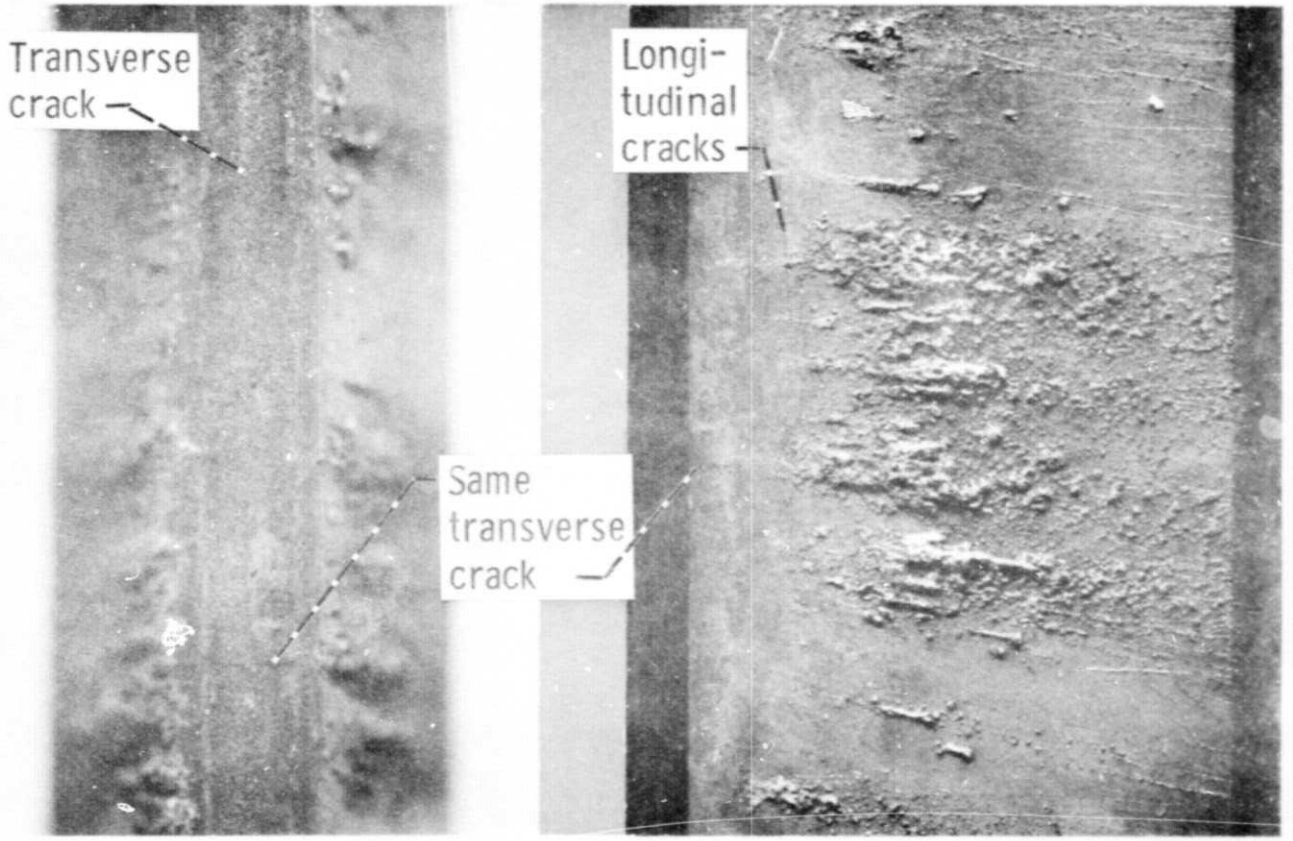

(a) Front view.

(b) Side view.

Figure 18. - Norton NC-435 siliconized SiC batch 1 vane hot zone leading edge after 1370^{0} C exposure for 19 cycles in Mach 1 burner rig, X10.